Distribution of membranes and the cytoskeleton during cell plate formation in pollen mother cells of *Tradescantia*

CHRISTEL R. SCHOPFER and PETER K. HEPLER

Department of Botany, and the Program in Molecular and Cellular Biology, University of Massachusetts, Amherst, MA 01003, USA

Summary

The cellular pattern and distribution of membranes have been analyzed during cytokinesis in pollen mother cells of *Tradescantia* and compared with those of actin microfilaments (MFs) and microtubules (MTs). Membranes have been stained with $DiOC_6(3)$ and MFs with rhodamine-labeled phalloidin (RP); analysis has been carried out on the confocal laser scanning microscope. MTs have been visualized as birefringent elements in the polarized light microscope. The results show that when the interzone first appears in mid anaphase it contains an even distribution of membranes. However, by late anaphase these elements have been cleared away, leaving the interzone largely devoid of $DiOC_6(3)$-positive material. MTs are found throughout this zone, while MFs appear in two non-overlapping sets on both sides of the cell equator. Thereafter membrane elements reappear in the interzone, but only along the equatorial line of the forming cell plate. Presumably these equatorial elements are composed of endoplasmic reticulum and Golgi vesicles, since the larger organelles, including amyloplasts and mitochondria, are excluded from the phragmoplast. MFs, like MTs, arrange preferentially normal to the cell plate, forming a dense array on both sides, but being absent from the zone occupied by the membranes. By contrast, the parallel set of MTs, while excluding larger organelles from the phragmoplast, intermingle with the membrane elements in the cell equator. As cytokinesis proceeds membranes continue to concentrate on the cell plate as indicated by its marked increase in staining with $DiOC_6(3)$. From a consideration of spatial and temporal organization of the phragmoplast components it is reasonable to suggest that both cytoskeletal components participate in the aggregation of vesicles that give rise to the cell plate. Membranes, on the other hand, through the provision of surface binding sites and/or through the regulation of the cytoplasmic calcium ion concentration, might be involved in the assembly and stabilization of the cytoskeleton.

Key words: membranes, microtubules, microfilaments, cell plate.

Introduction

The structure, composition and global architecture of the phragmoplast in dividing plant cells is becoming well characterized through analyses that have involved several different microscope techniques (Gunning, 1982; Seagull, 1989; Baskin and Cande, 1990). Microtubules (MTs), which comprise the most prominent element within the phragmoplast, for example, are known to exist in two overlapping (Hepler and Jackson, 1968) and oppositely polarized (Euteneuer *et al.* 1982) sets that are oriented normal to the developing cell plate. MTs arise initially from the interzone during anaphase and retain a close association with the edges of the centrifugally growing phragmoplast, finally disassembling at the completion of cell plate formation (Gunning, 1982). More recently actin microfilaments (MFs) have been identified as a component of the phragmoplast (Clayton and Lloyd, 1985; Gunning and Wick, 1985; Kakimoto and Shibaoka, 1987; Palevitz, 1987; Seagull *et al.* 1987; Traas *et al.* 1987; Sheldon and Hawes, 1988; Traas *et al.* 1989; McCurdy and Gunning, 1990; Cho and Wick, 1991; for reviews see Staiger and Schliwa, 1987; Lloyd, 1989; Wick, 1991). Although MFs are less well characterized than MTs, the available evidence indicates that they occupy a similar zone and may be oriented parallel to the MTs.

A third major component of the phragmoplast is the membranes. Vesicles derived from the Golgi dictyosomes aggregate and fuse to form the cell plate proper, while elements of tubular endoplasmic reticulum (ER) construct a network that appears to enmesh Golgi vesicles and may help control fusion processes (Gunning, 1982; Hepler, 1982). Although considerable information about the detailed structure of the phragmoplast membranes has been gleaned from ultrastructural studies, much less is known about their global architecture, their development during cell plate formation, or their relationship with MTs and MFs.

The purpose of this study is to provide a whole-cell structural analysis of membranes during phragmoplast formation and to compare their pattern and changes in distribution with MTs and MFs. Because of problems with artifacts during preparative staining procedures (Wick, 1991), great care has been taken to produce a minimum of perturbation from the living state. The membranes have been stained with $DiOC_6(3)$ under conditions of either light fixation or no fixation at all (McCauley and Hepler, 1990). MFs have been analyzed using rhodamine–phal-

Journal of Cell Science 100, 717–728 (1991)

loidin (RP) in cells that have only received a MF stabilization treatment and no fixation. Both membranes and MFs have been imaged in the confocal laser scanning microscope, which provides excellent resolution due to its ability to optically section fluorescently stained cells. Finally, MTs have been analyzed in living cells using polarized light microscopy (Inoue, 1986). The cell type analyzed throughout this study has been the pollen mother cell (PMC) of *Tradescantia* undergoing its first meiotic division.

Materials and methods

Materials

Tradescantia virginiana plants were grown in a growth chamber at 25°C with a 18 h photoperiod. Young inflorescences were chosen, and buds about six or seven from the open flower were carefully removed. One anther of each bud was squashed into isotonic medium containing 6.6% sucrose (Sigma), 30 mM Mes, pH 6.7. The developmental stage of the released PMCs was determined using Nomarski differential interference contrast optics (DIC); in general, two of the remaining five anthers were at the same stage. Thereafter, anthers with PMCs in late anaphase or telophase of the first meiotic division were cut open with extreme care. The stamen, submersed in a drop of the respective preparation solution, was held in place by its filament while one pollen sac was gently slit open with the tip of a sharp dissecting blade. It is important to apply only minimal pressure to the pollen sac, since PMCs are extremely sensitive to any kind of disruption. PMCs were released from the pollen sac by gently moving the open anther through the medium.

Membrane staining

PMCs were released directly into fixation solution containing 3% freshly prepared paraformaldehyde, 30 mM Pipes, 5 mM EGTA, and fixed for 10–30 min. Compared with 2% glutaraldehyde, paraformaldehyde fixation was faster and yielded lower background fluorescence. The carbocyanine dye 3,3′-dihexyloxacarbocyanine iodide ($DiOC_6(3)$, Eastman Kodak) was prepared from a stock solution in DMSO (dimethyl sulfoxide; 2.5 mg ml^{-1}) and then added to the cell suspension for a final concentration of 2.5 mg ml^{-1} in 0.1% DMSO. The cells were incubated until the PMCs were well stained (10–30 min) as judged by epifluorescence. The cells were mounted by mixing with agarose solution (Sigma type VII) to a final concentration of 0.2%.

Microfilament staining

Owing to the extreme sensitivity of MFs to aldehyde fixatives (1% fresh paraformaldehyde in 30 mM Pipes, 5 mM EGTA caused fragmentation of MF bundles within 10 min), non-fixed PMCs were used. MF bundles were stabilized with the crosslinking agent *m*-maleimidobenzoyl *N*-hydroxysuccinimide ester (MBS, Pierce) in the extraction medium (Sonobe and Shibaoka, 1989). Complete MF stabilizing medium, which was modified from Cho and Wick (1991), consisted of PMEG buffer (30 mM Pipes, pH 6.9, 5 mM EGTA, 2 mM $MgSO_4$, 1% polyethylene glycol), 0.05% Triton X-100, 0.01% Nonidet P40, 1% DMSO, 3 mM dithiothreitol, 40 μM leupeptin, 14 μM pepstatin, 6 mM phenylmethylsulfonyl fluoride and 0.1 mM MBS. RP stock solution in methanol (Eastman Kodak) was added to the complete stabilizing medium or applied subsequently in medium minus MBS (0.1 μM final concentration of RP and 0.3% methanol). Equivalent results were obtained when the stabilization medium was applied either prior to or simultaneously with staining with RP. The latter procedure was used in order to reduce the time between preparation and observation. After incubation for 10 min, PMCs were washed in PMEG buffer, attached to a polylysine-coated coverslip and mounted in buffer plus 2% *n*-propyl gallate (Sigma) as an antifading agent.

Birefringence of microtubules

PMCs were suspended in a drop of culture medium (30 mM Mes, 5 mM EGTA, 2 mM $MgSO_4$, 6.6% sucrose (Sigma) and allowed to settle onto a polylysine-coated coverslip. Excess fluid was wicked away so that the PMCs were covered by just a thin film of medium. The coverslip was mounted upside down onto a moisture chamber consisting of a slide in which a hole was drilled, and sealed on the bottom by a coverslip.

Microscopy

PMCs stained with $DiOC_6(3)$ or RP were viewed with the confocal laser scanning microscope (MRC 500 or MRC 600, Biorad Microscience Division), using the appropriate filter cubes, 488 nm for $DiOC_6(3)$, and 514 nm for RP. The laser light was attenuated with the neutral density filter wheel at its lowest setting and the pinhole closed as far as possible. Images were recorded using a 60× oil-immersion lens (NA 1.4), averaging 10–30 scans (Kalman filter), then contrast-enhanced on the Image 1/AT (Universal Imaging Corporation, West Chester, PA) and photographed from the monitor with a 35 mm Nikon camera using TMAX 400 film.

For visualization of the birefringence of phragmoplast MTs, we used a polarization microscope (Reichert) equipped with a strain-free objective lens (40×, NA 0.65, Olympus), a 1/30 λ Brace-Kohler compensator, a mercury vapor lamp, and a rotating stage. Images from a Dage-MTI (Michigan City, IN) series 65 video camera were processed on the Image 1/AT. The long axis of the cell was oriented at 45° to the axis of polarizer and analyzer, the compensator was rotated to either add (brighten) or subtract (darken) to the retardation effect of the object, thereby enhancing the contrast between the birefringent object and the background. Subsequent image processing, performed on the Image 1/AT, involved removal of background imperfections and enhancement of the contrast. The retardation of the phragmoplast was estimated according to Inoue (1986): (retardation of specimen)= (retardation of compensator)×sin(2ϑ).

Nomarski DIC images of living PMCs were taken by exchanging the compensator for a Nomarski prism and attenuating the light source.

Results

Techniques

This study sought to minimize the impact of experimental conditions on membrane elements, MFs and MTs. Membranes are well preserved with freshly prepared paraformaldehyde. By contrast, actin microfilaments are fragmented by aldehyde fixation, even when 3% paraformaldehyde is applied simultaneously with RP or when fixation was attenuated to 1% for 10 min. Treatment of non-fixed cells with MBS in the extraction medium for 10 min prior to or simultaneously with RP staining retained MF structure and permitted the observation of MFs in fine detail, not only in the phragmoplast but also in fibers in the spindle apparatus and a network in the cortical cytoplasm. Although MBS may have induced some polymerization of MFs onto existing bundles (Wick, 1991), this is thought to be minor, given the dramatic temporal and spatial changes in MF organization that clearly correlate with the particular stage of cell plate formation. The overall changes in MF distribution as described below are thought to represent the situation in a living cell.

A considerable effort has been made to use immunofluorescence to portray MTs. We find, however, that MTs are significantly perturbed by glutaraldehyde or paraformaldehyde even in the presence of the MT-specific crosslinking agent ethyleneglycol-bis-succinimidylsuccinate prior to fixation. An alternative technique employs the birefringent properties of the ordered MT arrays in the spindle apparatus and phragmoplast (Inoue and Bajer, 1961; Bajer, 1968). Fortunately the cell wall of the PMC is composed of callose and not cellulose, and therefore is only

weakly birefringent. *Tradescantia* PMCs contain a large number of birefringent amyloplasts, which obscure the image of metaphase spindles to some extent, but these organelles are excluded from the phragmoplast, making polarization microscopy a suitable technique for visualizing MTs in living PMCs undergoing cell plate formation. The compensator setting was chosen to show the birefringent MTs as brighter than the background (Inoue & Bajer, 1961).

Cell plate formation

The progress through cell plate formation has been divided into four major stages: (1) initiation of cytokinesis, (2) young phragmoplast, (3) mature phragmoplast, (4) disintegration of the phragmoplast. The organization of the three main constituents of the phragmoplast, membranes, MFs and MTs, are compared at each stage.

Initiation of cytokinesis. During anaphase, as the chromosomes move to the poles, an interzone emerges that is largely devoid of organelles or clearly identifiable structures when observed with Nomarski DIC optics (Fig. 1A,B). Staining with $DiOC_6(3)$, however, reveals that initially the interzone contains numerous membrane elements that are dispersed throughout (Fig. 1C). As anaphase progresses and the chromosomes reach the poles, these membrane elements are removed from the interzone. The larger organelles, mainly amyloplasts and mitochondria, become concentrated in the cortical cytoplasm or appressed to the proximal side of the decondensing chromosomes (Fig. 1A,B).

At this stage, MFs undergo a major rearrangement. In late anaphase, RP staining shows numerous thin MF bundles throughout the interzone (Fig. 1E). Subsequently, they increase dramatically, showing a preferred orientation perpendicular to the cell equator (Fig. 1F). MTs also increase sharply in the interzone. During mid-anaphase chromosome-to-pole fibers are still evident (Fig. 1G), but these disassemble and by late anaphase a distinctly birefringent interzone emerges (Fig. 1H).

Young phragmoplast. Within the interzone a thin line appears, as observed by Nomarski DIC, that marks the inception of the cell plate (Fig. 2A,B). Although the interzone has been largely swept clear of all $DiOC_6(3)$-positive material, note that a faint staining begins to appear in the equatorial plane (Fig. 2C), and that this staining increases as cell plate development proceeds (Fig. 2D). We presume that these images are due to the presence of Golgi vesicles and elements of ER that specifically align in the region of the plate, while the larger organelles, such as plastids and mitochondria, remain in the cortical cytoplasm, or appressed to the cytoplasmic surfaces of the re-forming nuclei.

RP staining shows a marked accumulation of MF bundles on both sides of the membrane plate, but it is particularly noteworthy that these bundles usually do not cross the zone occupied by the membranes themselves. Thus, in RP-stained phragmoplasts, one always observes a dark line that corresponds to the cell plate itself. MF bundles initially occupy a cylindrical volume in the center, and subsequently shorten along the cell axis, while expanding centrifugally towards the periphery (Fig. 2F). Only a few thin MF bundles can be detected outside the phragmoplast, and these usually reside in the cell cortex.

MTs undergo a rearrangement similar to that of the MF array in the interzone; they shorten to form a broad disc that expands centrifugally (Fig. 2G,H). However, MTs are longer than MFs, and by contrast cross the zone occupied by the cell plate membranes. Within the phragmoplast MTs one can observe a thin, weakly birefringent line at the equatorial plane (Fig. 2H) that corresponds to the alignment of the young cell plate noted by Nomarski DIC (Fig. 2B) and fluorescence microscopy (Fig. 2D). Although both MTs and MFs could contribute to the exclusion of larger organelles from the cytokinetic apparatus, we believe that MTs dominate this activity. MTs are longer than MFs and their location more corresponds closely than MFs to the region from which the larger organelles are absent.

Mature phragmoplast. As development proceeds (Fig. 3A–H) aggregating vesicles coalesce to form a well-defined cell plate (Fig. 3A). Through the addition of new vesicles at its centrifugal edges, the plate expands and finally makes contact with the parent cell wall (Fig. 3B). $DiOC_6(3)$ staining shows that the membrane elements of the plate, which are at first more loosely organized (Fig. 3C), become consolidated into a tight and brightly stained structure that extends completely across the cell (Fig. 3D). At the edge where the plate contacts the parental wall it is quite thin, as depicted by $DiOC_6(3)$ staining (Fig. 3C,D), whereas in central sections the membrane complex of the plate is much thicker (Fig. 3C,D).

In Fig. 4A–H a series of optical sections from the cell shown in Fig. 3C reveals in greater detail the distribution of membranes between the central region of the plate and its developing edges. Medial sections (Fig. 4A–D) indicate that the bulk of the cell plate at this stage has a thickened appearance due to the somewhat loose organization of membrane elements. As the optical sections approach the edge of the cell (Fig. 4E–H) the plate itself becomes progressively thinner until it is evident only as a faintly fluorescent line (Fig. 4H). This sequence also emphasizes the fact that the large organelles, especially the amyloplasts, are confined to the cell cortex, but not in that zone to which the phragmoplast is directed and where the cell plate will fuse with the parental wall.

MFs show a structural pattern that is complementary to the membranes above. Flanking both sides of the membrane plate, the array of MF bundles shortens and extends across the diameter of the cell plate (Fig. 3E,F). Again, notice that MF bundles are almost completely absent from the zone occupied by the aggregating membrane plate. MTs continue to show a pattern that is similar in distribution to that of MFs (Fig. 3G,H), with two important exceptions: they are longer than MFs and in some instances (for example, Fig. 3G) they can be observed to traverse the zone occupied by the membrane elements in the cell plate. Measurement of the average birefringent retardation of the aligned MTs in mature phragmoplasts yields values between 3 and 3.6 nm.

Disintegration of the phragmoplast. In the terminal stages of cytokinesis a distinct, continuous, although often wavy, cell plate is evident throughout the cell equator (Fig. 5A,B,C,E,G). Although the distinctions between cells with maturing phragmoplasts and those with disintegrating phragmoplasts are subtle, they are nevertheless evident. For example, in disintegrating phragmoplasts the plate itself, as revealed by Nomarski DIC optics, has become quite thickened (compare Fig. 3A,B with 5A,B), a condition that is similarly borne out by the more intense and thickened region of staining with $DiOC_6(3)$ (compare Fig. 3C,D with 5C,D). In late stages when the two cells begin to separate from one another, clefts form at the cell edge (Fig. 5D), and these, in contrast to the still adjoined

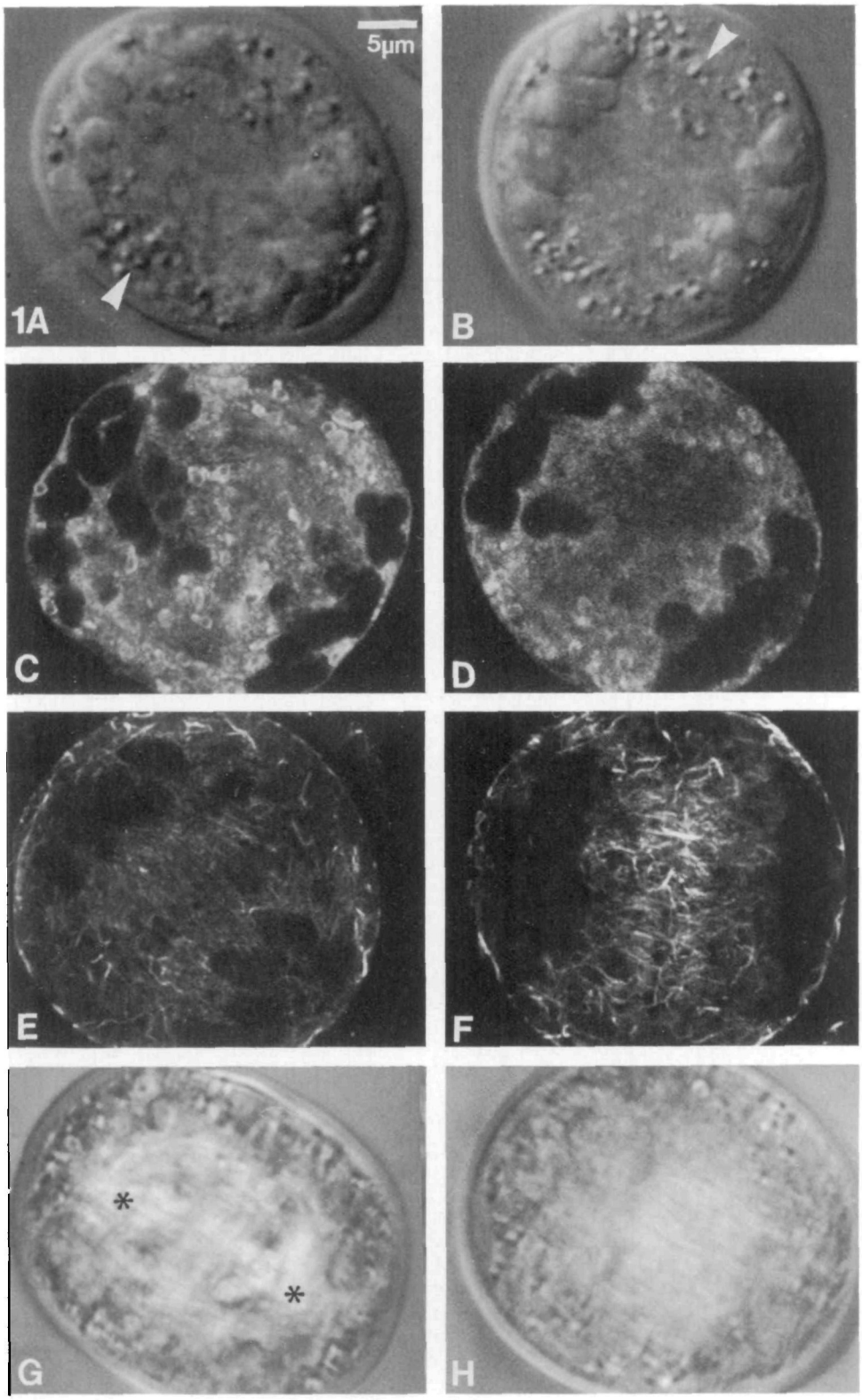

Fig. 1. (A–H) Initiation of cytokinesis at late anaphase. (A,B) Nomarski DIC images of living PMCs show that the meiotic apparatus occupies most of the cell volume; the larger organelles, such as amyloplasts (arrowheads), are confined to the edges of the cell. (C,D) $DiOC_6(3)$ staining of cells at the same stage as those shown in A,B shows that the membrane elements are initially rather evenly spread throughout the cell (C), but that as anaphase progresses they diminish in amount in the interzone and accumulate in the cell cortex and in association with the surfaces of the condensing chromosomes (D). (E,F) RP staining reveals that MFs at first are rather loosely distributed across the interzone (E), but, by contrast with the membranes, they begin to accumulate in the interzone as development proceeds (F). (G,H) Polarized light microscopy indicates the distribution of MTs. In mid-anaphase (G) chromosome-to-pole birefringence is evident (asterisks, G); however, later (H), when the chromosomes approach the poles, the marked birefringence of the interzone indicates a high degree of MT organization in this region. Bar, 5 μm. ×1700.

new wall, show relatively little fluorescence. The new wall is birefringent (Fig. 5G,H), which may be due to ordered material within the wall itself, or to the parallel alignment of cytoplasmic structures such as MTs and/or lamellar ER.

The cytoskeleton, including both MFs (Fig. 5E,F) and MTs (Fig. 5G,H) depolymerizes, normally in a centrifugal pattern. This process is well known for MTs and is shown in Fig. 5G, where birefringence is diminished from the central region of the plate while still strong at its edges. A similar sequence in degradation holds for the MFs as well. Fig. 6A–D shows a RP-stained mature phragmoplast in an obliquely oriented cell, which reveals that the MFs extend completely across the cell. In a later stage, also from an

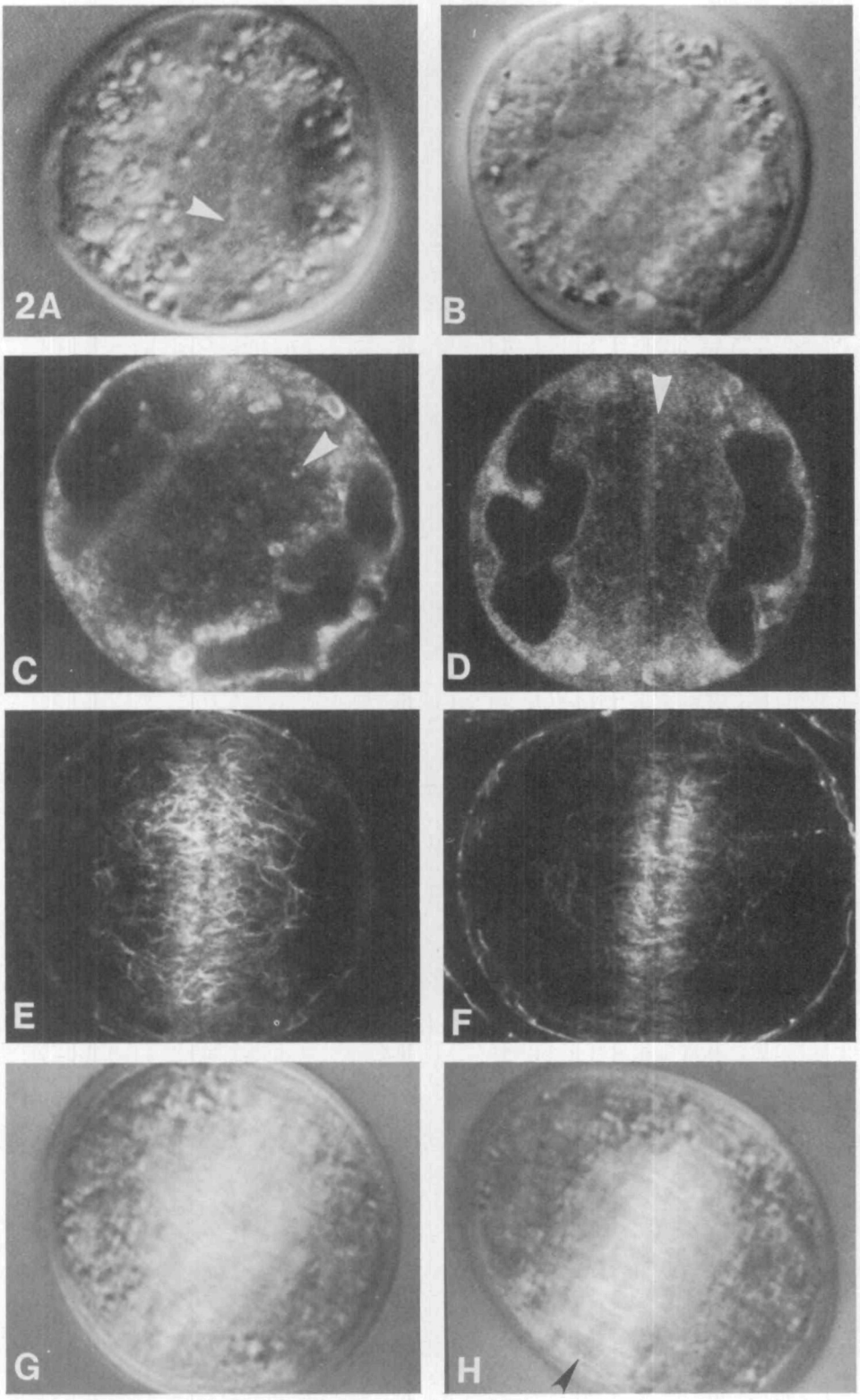

Fig. 2. (A–H) Young phragmoplast. (A,B) Nomarski DIC images of living cells shows the first sign of plate formation in the cell equator (arrowhead, A). At a slightly later stage (B), the plate is visible as a disc that extends across the interzone. (C,D) $DiOC_6(3)$ staining indicates that membrane elements, although largely eliminated from the interzone, start to accumulate as nodules in the equatorial plane (arrowhead, C) and later align in a more complete and well-oriented plane (arrowhead, D). The large organelles remain in the cortical cytoplasm or appressed to the surface of the re-forming nuclei. (E,F) RP staining shows that the number of MFs near the plate increases dramatically. MFs are oriented preferentially normal to the equator, and, with only a few exceptions, do not pass through the plane of the plate. (G,H) Polarized light microscopy indicates that the array of birefringent MTs in the interzone becomes shorter and expands towards the periphery (compare G and H). In H, a faint line (arrowhead), which is more weakly birefringent than the bulk interzone, represents the early membrane plate. ×1700.

obliquely oriented cell, the MFs in the central region of the cell plate have broken down, leaving only those at the circumference (Fig. 7A,B), which now appear as a wreath.

Discussion

Membrane elements constitute a conspicuous component of the cell plate. However, their association with the phragmoplast is complex (Fig. 8A–D). Initially, when the interzone first emerges during mid-anaphase, there are membranes throughout. But by late anaphase these are swept out of the interzone, perhaps by the forming palisade of phragmoplast MTs (Fig. 8A). Membranes then reappear, and are evident as part of the developing cell

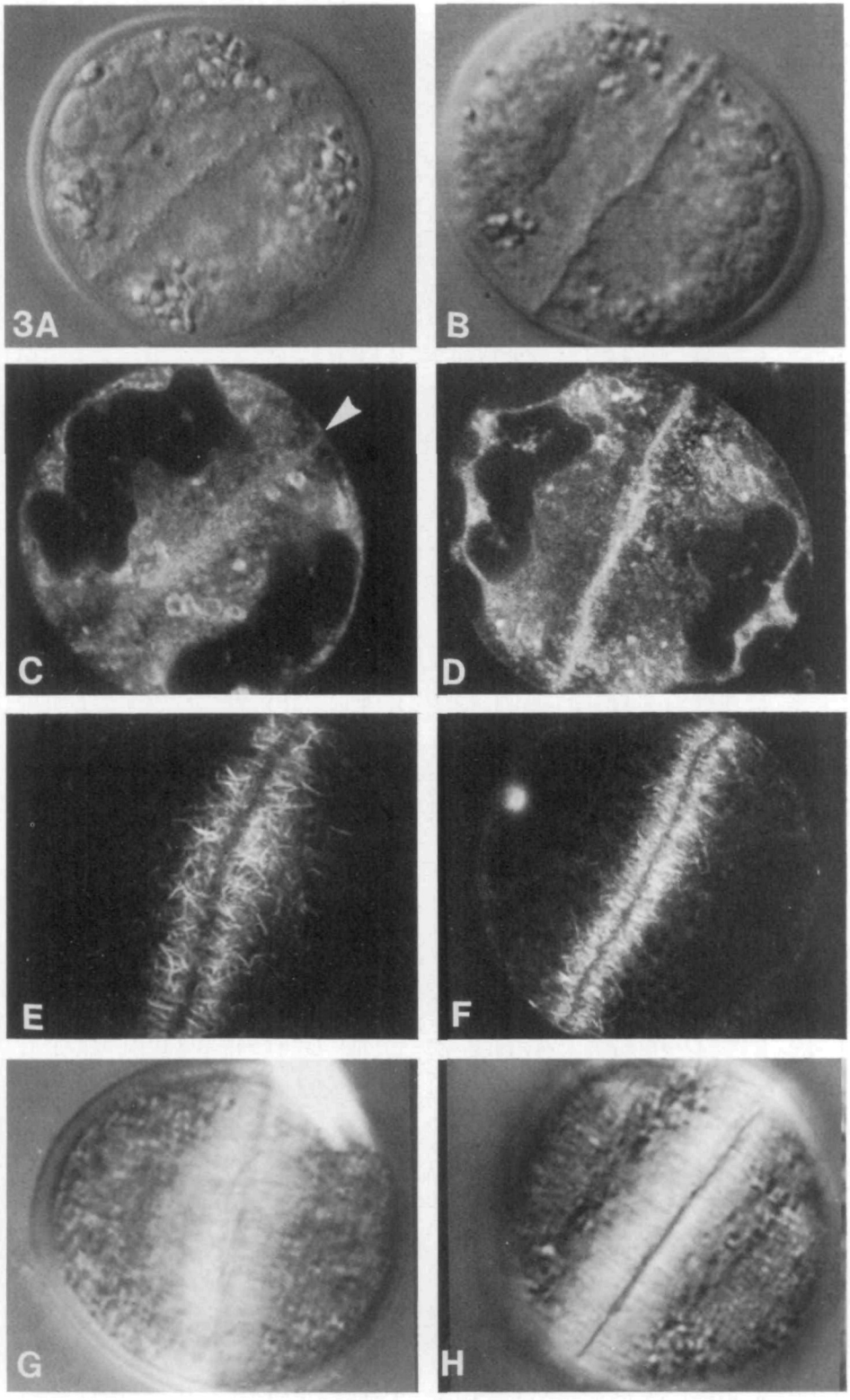

Fig. 3. (A–H) Maturation of the phragmoplast. (A,B) Nomarski DIC images show a distinct plate in the cell equator that extends across the entire cell (B), contacting the parental cell wall. (C,D) $DiOC_6(3)$ staining indicates that the membrane plate becomes progressively consolidated. Note, especially in D, that whereas the plate itself is intensely stained the regions immediately flanking both sides have a greatly reduced density of membranes. As the plate extends centrifugally to the edges of the cell its distal, more newly formed, regions are thin compared to the central portions (arrowhead, C). Also note that the larger organelles have now been swept out of this portion of the cortical cytoplasm (compare A,B with C,D). (E,F) RP staining shows a dense array of short MF bundles arranged on both sides of the membrane plate, but conspicuously absent from the plate region itself. (G,H) Polarized light microscopy reveals that the array of shortened MTs forms a continuous disc in the cell equator. MTs extend into the zone occupied by membranes. The dense palisade of MTs, being longer and more strictly organized than MFs, effectively excludes amyloplasts from the cytokinetic apparatus, and appears to be responsible for clearing the cortical cytoplasm at the zone of cell plate–parental wall contact (H). The extremely briefringent material in the upper part of G is an oxalate crystal that unfortunately imposed itself. ×1700.

plate confined to the equatorial plane of the interzone (Fig. 8B,C). As known from EM studies (Hepler and Newcomb, 1967; Schmiedel *et al.* 1981; Gunning, 1982; Hepler, 1982; Nakamura and Miki-Hirosige, 1988), these membrane elements are composed of ER and Golgi vesicles that aggregate in a discrete plane where the two arrays of MTs overlap (Hepler and Jackson, 1968). The larger organelles, e.g. amyloplasts, however, are completely excluded. As the phragmoplast disintegrates, the well-defined plate of membrane elements persists, and even increases, perhaps to account for the thickening of the cell wall that arises in this zone (Fig. 8D). These observations augment those previously made from EM studies and provide a more complete impression of the source, specific location and dynamics of membrane elements that contribute to cell plate formation.

MFs are a consistent component of the phragmoplast. In late anaphase, they concentrate in the interzone and later

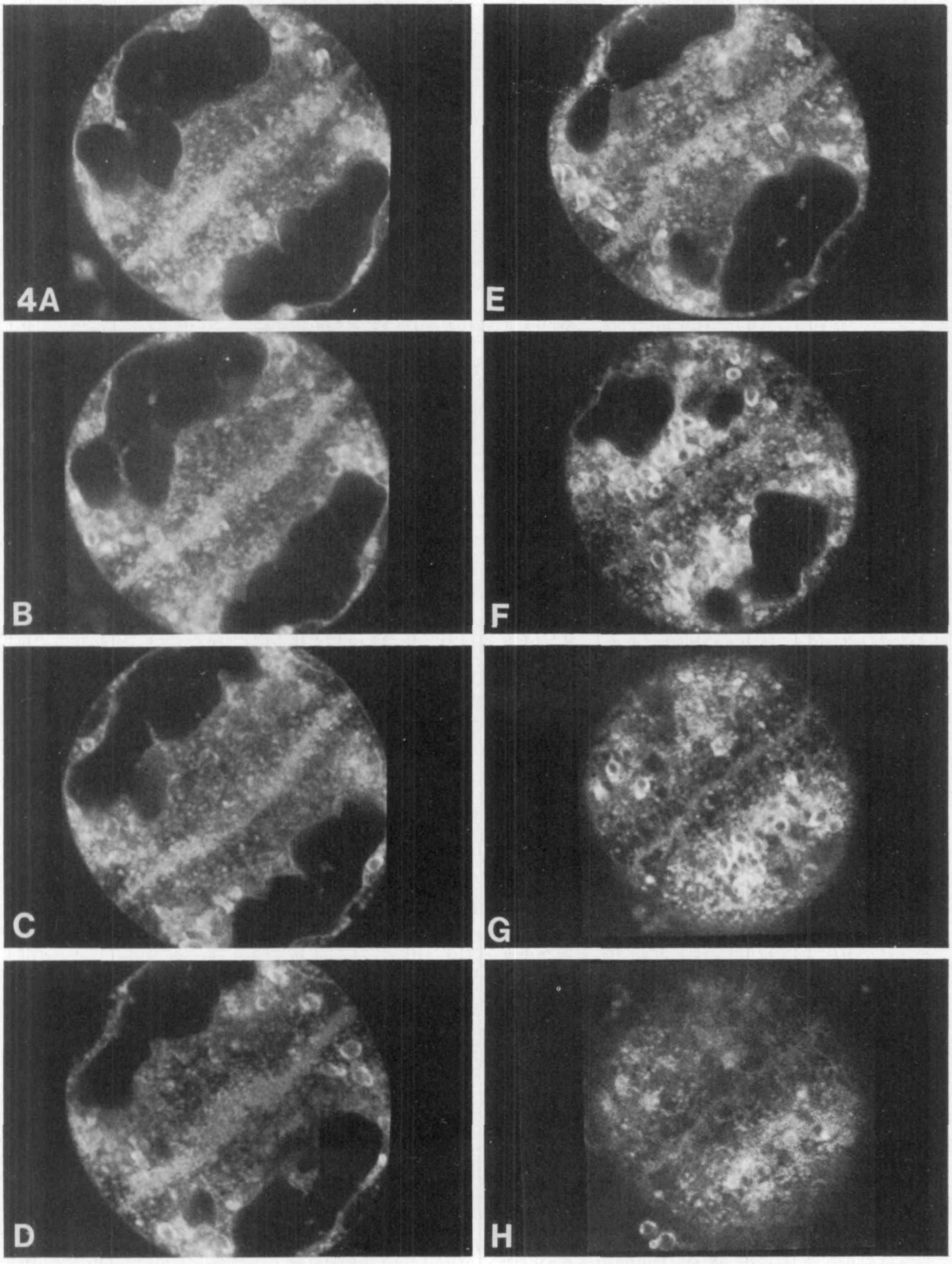

Fig. 4. (A–H) Serial optical sections of the same cell shown in Fig. 3C. Medial sections (A,B,C) show a dense accumulation of $DiOC_6(3)$-positive membrane elements in the cell equator. Towards the periphery, the membrane plate is thinner. Optical sections through the periphery (F, G, H) provide a face view of the thin line of membrane elements that comprise the plate near the cell edge. Focusing on the plasma membrane (H), the margin of the membrane plate contacting the plasma membrane can be seen.

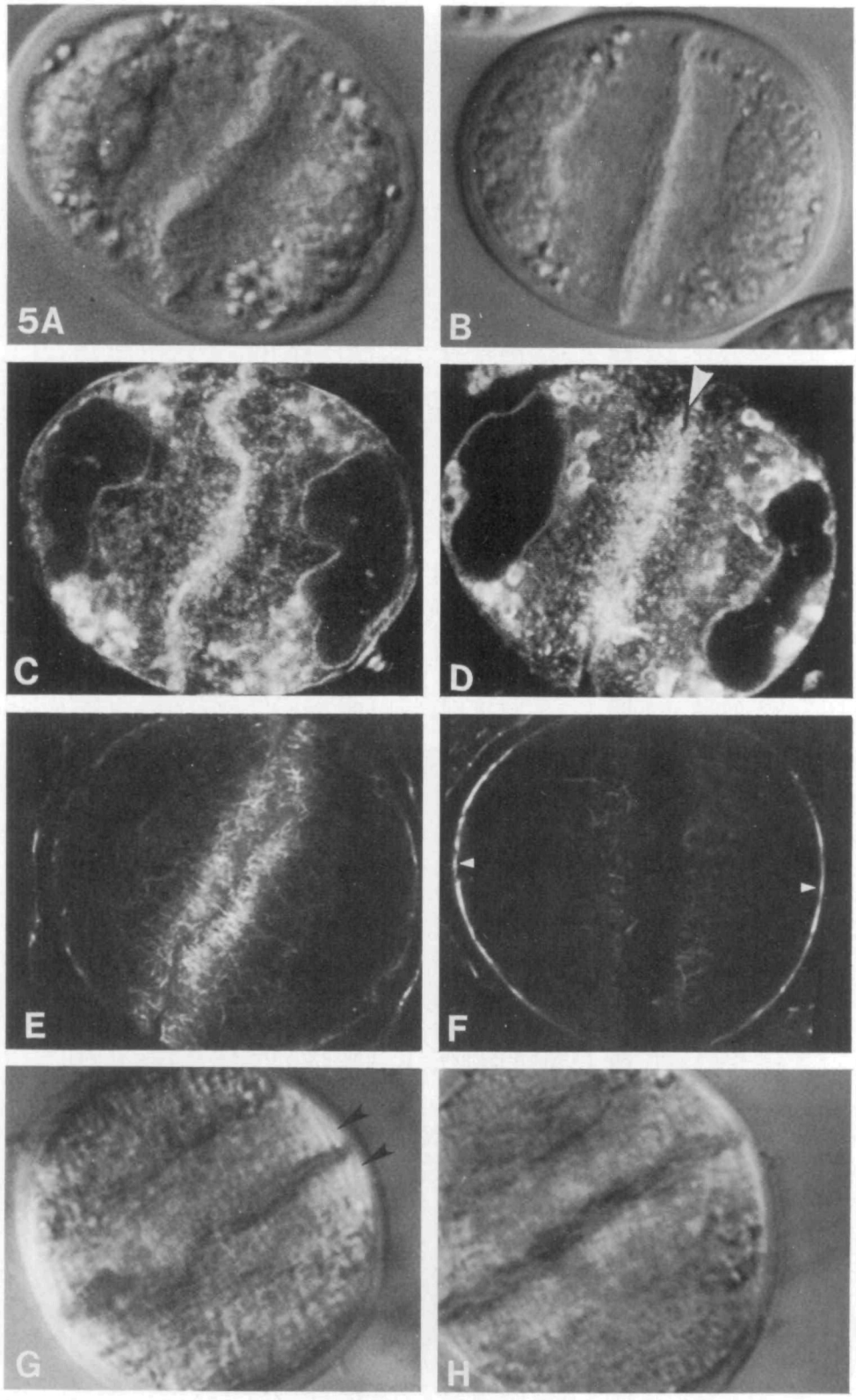

Fig. 5. (A–H) Disintegration of the phragmoplast.
(A,B) Nomarski DIC, as well as the other optical methods, reveals a thickened cell plate, although at this stage it may still be strongly wrinkled (A,C,E,G). Only later, the plate straightens (B, H) and forms a rigid structure. (C,D) $DiOC_6(3)$ staining shows that the membranes throughout the plate aggregate tightly. In D the two daughter cells are beginning to pull away from one another, creating small clefts at the cell margins (arrowhead, D).
(E,F) RP staining indicates that the MFs, formerly concentrated at cell plate (E), depolymerize at the completion of cytokinesis (F). Only a few weakly labeled MFs are detectable, whereas RP-positive material is observed at the cell cortex especially on the poleward surfaces of the cell (small arrowheads, F). (G,H). Polarized light microscopy shows the disintegration of the array of phragmoplast MTs. As shown in G, MTs first depolymerize in the central region, leaving a ring of MTs at the edge of the plate (arrowheads, G), which later also disappear (H). Note that the birefringence of the new cell wall (H) is opposite in sign to that of the phragmoplast MTs. ×1700.

form a dense array in which the individual elements are oriented preferentially normal to the membrane plate. Thus they are similar, but not identical, in distribution to MTs, being confined to a narrower zone flanking both sides of the plate. While some of the MFs may be derived from the array that penetrated or encaged the mitotic–meiotic apparatus (unpublished observations; and Schmit and Lambert, 1990), the massive accumulation at subsequent stages requires new polymerization of F-actin in the phragmoplast. This has been shown directly in endosperm cells (Schmit and Lambert, 1990) where a differentially labeled population of MFs arises in the cell plate.

A particularly noteworthy feature of our current investigation is the observation that MFs usually do not

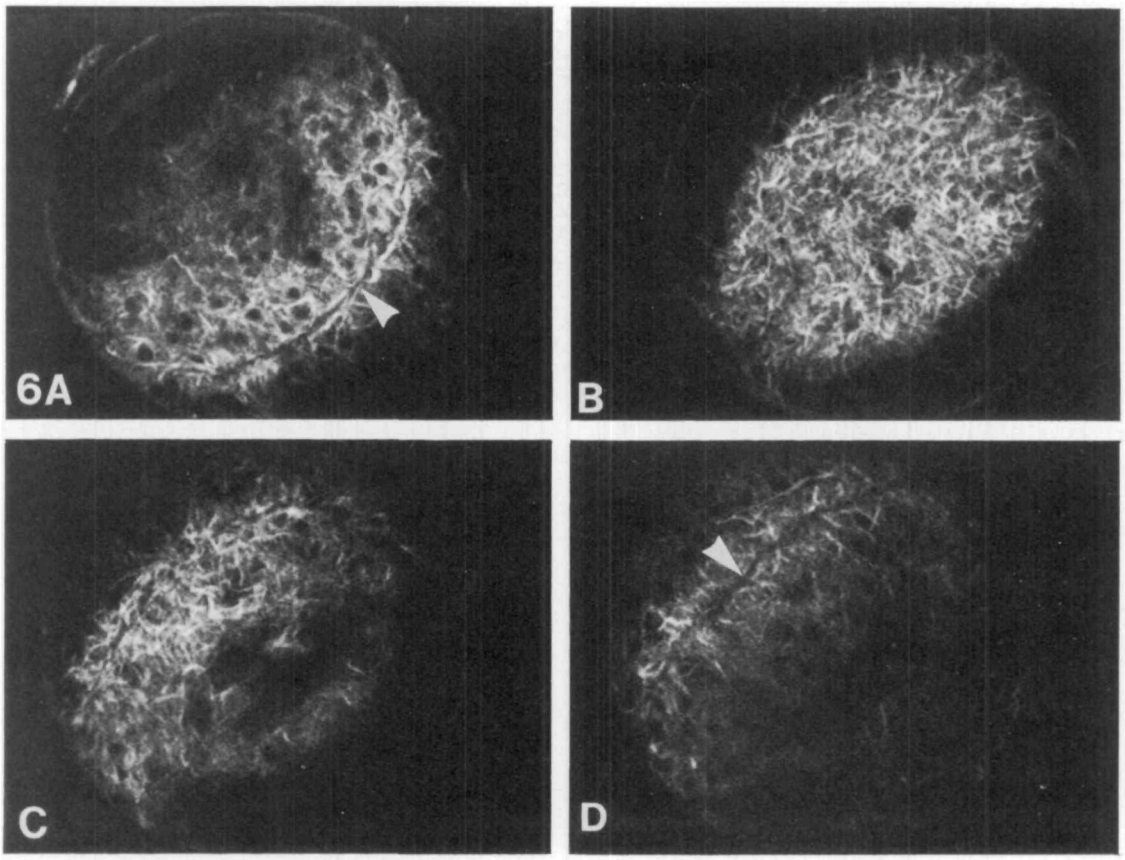

Fig. 6. (A–D) RP staining of mature phragmoplasts. Serial optical sections through a tilted phragmoplast show that at this stage MF bundles are present throughout the plane of the plate. B is an optical section through the central region of the MF array. Peripheral sections A and D show that MFs are oriented preferentially normal to the plate, and are absent from the narrow plane occupied by the membranes (arrowheads, A,D). ×1700.

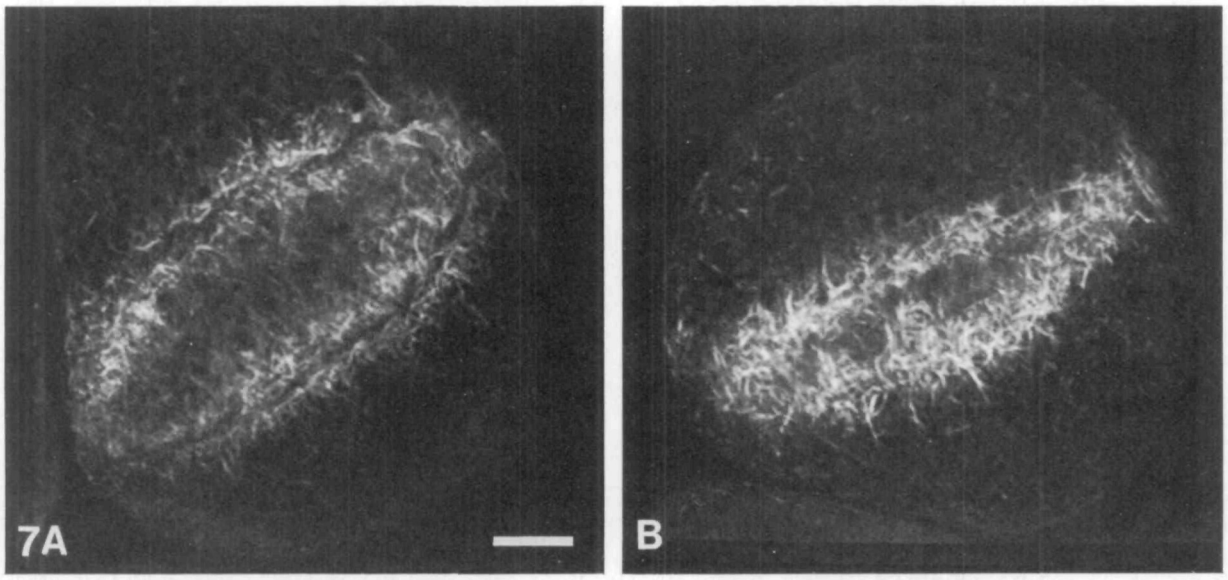

Fig. 7. (A,B) RP staining of a disintegrating phragmoplast. The oblique view shows that MFs in the central region of the phragmoplast are depolymerized, leaving a wreath-shaped array at the periphery of the equator. Bar, 5 μm. ×2000.

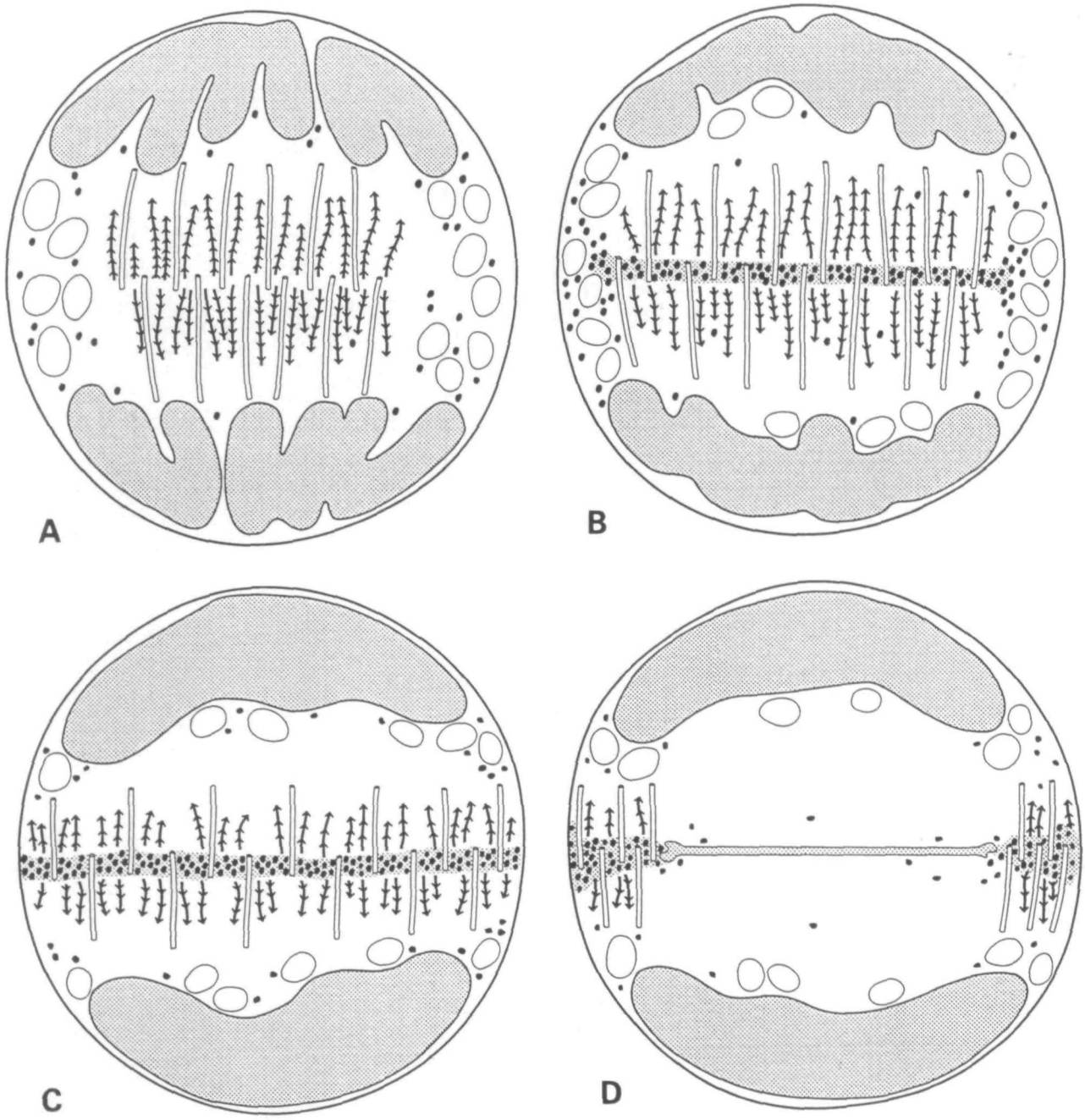

Fig. 8. (A–D) Summary diagrams show the pattern and distribution of membranes and the cytoskeleton during cell plate formation. (A) At late anaphase the interzone has been swept clear of most membranes; however, both MTs, depicted as tubules, and MFs, depicted as barbed fibers, become concentrated in this region. Amyloplast are pushed to the cortical regions of the cell. (B) As cytokinesis proceeds, membrane elements, including small vesicles and elements of ER, shown as small black dots and stippling, aggregate in the equatorial region of the interzone, giving rise to the young cell plate. Both MTs and MFs shorten in length, as the phragmoplast as a whole expands centrifugally towards the edges of the cell. (C) The growing cell plate extends to the edges of the cell. MTs and MFs occur throughout the width of the cell at this point. Notice that the amyloplasts have been cleared from those region of the cell cortex to which the growing cell plate is directed. (D) In late stages of cytokinesis membranes have consolidated in the central part of the plate, while vesicles still accumulate at its edges. MTs and MFs have depolymerized in the central region of the plate but are also present at the edges.

cross the plane of the plate. Some previous studies (Gunning and Wick, 1985; Kakimoto and Shibaoka, 1987; Palevitz, 1987; Seagull *et al.* 1987) show a dark line that corresponds to the cell plate, but have not reported the sharp discontinuity of RP staining at the cell plate noted herein, even in comparable cells such as PMCs of lily (Sheldon and Hawes, 1988) and eggplant (Trass *et al.* 1989). The use of the confocal microscope, by providing optical sections that are not confused by fluorescence above and below the plane of focus, may be responsible for the clarity of images produced herein. It is also possible that the images are misleading and that actin MFs indeed do extend into and through the plate like MTs. For example, when actin MFs are closely associated with membrane elements it is conceivable that they cannot be stained with RP. Other methods should be used, therefore,

to either confirm or reject the absence of MFs in the plane of the cell plate.

The striking and specific associations of MFs with the phragmoplast are augmented by several other studies showing the similar localization of related proteins including myosin (Parke *et al.* 1986), troponin T (Lim *et al.* 1986), an actin-associated calcium-dependent protein kinase (Putnam-Evans *et al.* 1989), and phosphoproteins (Vandre *et al.* 1986). Taken together these observations strongly indicate the involvement of an actomyosin-based transport system within the cytokinetic apparatus. Ultrastructural studies of phragmoplasts treated with heavy meromyosin also reveal a symmetrical distribution of MFs with the arrowheads pointing away from the plate (Kakimoto and Shibaoka, 1988). The MF polarity of the phragmoplast thus resembles that of actin on both sides of the Z disc in a muscle fiber. Interestingly, the motion of particles in the phragmoplast is towards the equatorial plane, as is the motion of myosin relative to the Z disc in muscle. Cytoplasmic streaming in plant cells is yet another example in which particles are propelled opposite to the direction of the arrowheads (Kersey *et al.* 1976). These observations are consistent with the idea that actin contributes to inward motion of Golgi vesicles during cell plate formation. The wreath-shaped array of MFs seen in disintegrating phragmoplasts (Fig. 7; Kakimoto and Shibaoka, 1987) is additionally consistent with this speculation, since it places the MFs at the growing margin, where active transport of vesicles occurs.

MTs are the most prominent component of the phragmoplast. They are partially derived from remnants of interzonal spindle (Fig. 1G). Zhang *et al.* (1990) showed directly in living cells, using fluorescently labeled tubulin as a probe for spindle and phragmoplast MTs, that a marked interzone apparatus always exists, but that its component MTs coalesce and increase in structural intensity with the formation of the phragmoplast. The transition involves new nucleation, which has been demonstrated for endosperm cells (Vantard *et al.* 1990) to occur mainly at the cell plate, where the plus ends of the MTs intermingle with the ER network and aggregating Golgi vesicles (Euteneuer *et al.* 1982).

It is reasonable to imagine that MTs, as well as MFs, participate in the movement of dictyosome vesicles into the cell plate. Although cell plates may appear abnormal in the presence of the actin-MF-modifying drug, cytochalasin (Palevitz and Hepler, 1974; Gunning and Wick, 1985; Venverloo and Libbenga, 1987; Cho and Wick, 1991), they usually form, indicating that motile elements besides MFs are probably functioning. The obvious candidates are the phragmoplast MTs. It is further interesting to speculate, given the known polarity of these MTs, that a plus-end-directed motor, possibly kinesin (Vale, 1987), generates the inward flow of dictyosome vesicles. Additional studies are needed to test this postulate and to determine further the relative contribution of actin-based and tubulin-based motile systems in the formation of the cell plate.

The close structural association between membranes and the cytoskeleton, especially MTs, in the plane of the plate invites speculation about possible functional relationships. The membranes could control the local calcium ion concentration and thereby promote MT assembly or disassembly (Hepler *et al.* 1990). This idea is strengthened by studies using chlortetracycline (Saunders and Hepler, 1981; Schmiedel *et al.* 1981), which indicate an increase in membrane-associated calcium in the region of the plate. In addition to a role in regulation of the local calcium level, membranes might provide a structurally defined locus that stabilizes new MT formation and assists in their growth (Hepler *et al.* 1990).

In summary, the distribution of membranes during cell plate formation can be closely correlated with the pattern of MFs and MTs. Membrane elements are concentrated in a distinct plane, from which MFs, based on RP staining, are absent. By contrast, the membranes enmesh with MTs in the equatorial zone where the latter are known to interdigitate at their plus ends. While there is reason to suspect that both cytoskeletal components contribute to membrane accumulation, it is also plausible that membranes contribute to the formation, stabilization and breakdown of the cytoskeleton.

We thank Dr S. Wick, University of Minnesota, for many helpful comments during the course of this research. We also thank our colleagues at University of Massachusetts, D. Callaham, S. Lancelle, M. McCauley, B. Rubinstein, P. Wadsworth and D. Zhang for many useful discussions and technical suggestions. We greatly appreciate the assistance provided by A. Hepler, M. Hepler and J. Whitehead in the preparation of the diagrams. This work was supported by grants from the USDA (88–37261–3727) and the NSF (DCB–88–01750).

References

Bajer, A. (1968). Fine structure studies on phragmoplast and cell plate formation. *Chromosoma* **24**, 383–417.

Baskin, T. I. and Cande, W. Z. (1990). The structure and function of the mitotic spindle in flowering plants. *A. Rev. Pl. Physiol. Pl. molec. Biol.* **41**, 277–315.

Cho, S. O. and Wick, S (1991). Actin in the developing stomatal complex of winter rye: a comparison of actin antibodies and Rh-phalloidin labeling of control and CB-treated tissues. *Cell Motil. Cytoskel.* (in press).

Clayton, L. and Lloyd, C. W. (1985) Actin localization during the cell cycle in meristematic plant cells. *Expl Cell Res.* **156**, 231–238.

Euteneuer, U., Jackson, W. T and McIntosh, J. R. (1982). Polarity of spindle microtubules in *Haemanthus* endosperm. *J. Cell Biol.* **94**, 644–653.

Gunning, B. E. S. (1982). The cytokinetic apparatus: its development and spatial regulation. In *The Cytoskeleton in Plant Growth and Development* (C. W. Lloyd, ed.) Academic Press, New York, NY, pp. 229–292.

Gunning, B. E. S. and Wick, S. (1985). Preprophase bands, phragmoplasts, and spatial control of cytokinesis. *J. Cell Biol. Suppl.* **2**, 157–179.

Hepler, P. K. (1982). Endoplasmic reticulum in the formation of the cell plate and plasmodesmata. *Protoplasma* **111**, 121–133.

Hepler, P. K. and Jackson, W. T (1968). Microtubules and early stages of cell plate formation in *Haemathus katherinae*. *J. Cell Sci.* **5**, 727–743.

Hepler, P. K. and Newcomb, E. (1967). Fine structure of cell plate formation in the apical meristem of *Phaseolus* roots. *J. Ultrastruct. Res.* **19**, 489–513.

Hepler, P. K., Palevitz, B A., Lancelle, S. A., McCauley, M. M and Lichtscheidl, I. (1990). Cortical endoplasmic reticulum in plants. *J. Cell Sci.* **96**, 355–373.

Inoue, I. (1986). *Videomicroscopy*. Plenum Press, New York.

Inoue, I. and Bajer, A. (1961). Birefringence in endosperm mitosis. *Chromosoma* **12**, 48–63.

Kakimoto, T. and Shibaoka, H. (1987). Actin filaments and microtubules in the preprophase band and phragmoplast of tobacco cells. *Protoplasma* **140**, 151–156.

Kakimoto, T. and Shibaoka, H. (1988). Cytoskeletal ultrastructure of phragmoplast-nuclei complexes isolated from cultured tobacco cells. *Protoplasma (Suppl.)* **2**, 95–103.

Kersey, Y. M., Hepler, P. K., Palevitz, B. A. and Wessells, N. K. (1976). Polarity of actin filaments in characean algae. *Proc. natn. Acad. Sci. U.S.A.* **73**, 165–167.

Lim, S. S., Hering, G. E. and Borisy, G. G. (1986). Widespread occurrence of anti-troponin T crossreactive components in non-muscle cells. *J. Cell Sci.* **85**, 1–19.

Lloyd, C. W. (1989). The plant cytoskeleton. *Curr. Opin. Cell Biol.* **1**, 30–35.

McCauley, M. M. and Hepler, P. K. (1990). Visualization of the

endoplasmic reticulum in living buds and branches of the moss *Funaria hygrometrica* by confocal laser scanning microscopy. *Development* **109**, 753–764.
McCurdy, D. W. and Gunning, B. E. S. (1990). Reorganization of cortical actin microfilaments and microtubules at preprophase and mitosis in wheat root-tip cells: A double label immunofluorescence study. *Cell Motil. Cytoskel.* **15**, 76–87.
Nakamura, S. and Miki-Hirosige, N H. (1982). Coated vesicles and cell plate formation in the microspore mother cell. *J. Ultrastruct. Res.* **80**, 302–311.
Palevitz, B. A. (1987). Accumulation of F-actin during cytokinesis in *Allium*. Correlation with microtubule distribution and the effects of drugs. *Protoplasma* **141**, 24–32.
Palevitz, B. A. and Hepler, P. K. (1974). The control of the plane of division during stomatal differentiation in *Allium*. II. Drug studies. *Chromosoma* **46**, 327–341.
Parke, J., Miller, C. and Anderton, B. H. (1986). Higher plant myosin heavy-chain identified using a monoclonal antibody. *Eur. J. Cell Biol.* **41**, 9–13.
Putnam-Evans, C., Harmon, A. C., Palevitz, B. A., Fechheimer, M. and Cormier, M. J. (1989). Calcium-dependent protein kinase is localized with F-actin in plant cells. *Cell Motil. Cytoskel.* **2**, 12–22.
Saunders, M. J. and Hepler, P. K. (1981). Localization of membrane-associated Ca^{2+} following cytokinin treatment in *Funaria* using chlorotetracycline. *Planta* **152**, 272–281.
Schmiedel, G., Reiss, H. D. and Schnepf, E. (1981). Association between membranes and microtubules during mitosis and cytokinesis in caulonema tip cells of the moss *Funaria hygrometrica*. *Protoplasma* **108**, 173–190.
Schmit, A. C. and Lambert, A. M. (1990). Microinjected fluorescent phalloidin *in vivo* reveals F-actin dynamics and assembly in higher plant cell. *Pl. Cell.* **2**, 129–138.
Seagull, R. W. (1989). The plant cytoskeleton. *Crit Rev. Pl. Sci.* **8**, 131–167.
Seagull, R. W., Falconer, M. M. and Weerdenburg, C. A. (1987). Microfilaments: dynamic arrays in higher plant cells. *J. Cell Biol.* **104**, 995–1004.
Sheldon, J. M. and Hawes, C. (1988). The actin cytoskeleton during male meiosis in *Lilium*. *Cell Biol. Int. Rep.* **12**, 471–477.
Sonobe, S. and Shibaoka, H. (1989). Cortical fine actin filaments in higher plant cells visualized by rhodamine-phalloidin after pretreatment with *m*-maleimidobenzoyl *N*-hydroxisuccinimide ester. *Protoplasma* **148**, 80–86.
Staiger, C J. and Schliwa, M. (1987). Actin localization and function in higher plants. *Protoplasma* **141**, 1–12.
Traas, J., Burgain, S. and Dumas de Vaulx, R. (1989). The organization of the cytoskeleton during meiosis in eggplant (*Solanum melongena* L)): microtubules and F-actin are both necessary for coordinated meiotic division. *J. Cell Sci.* **92**, 541–550.
Traas, J., Doonan, J. H., Rawlins, D. J., Shaw, P. J., Watts, J. and Lloyd, C. W. (1987). An actin network is present in the cytoplasm throughout the cell cycle of carrot cells and associates with the dividing nucleus. *J. Cell Biol.* **105**, 387–395.
Vale, R. D. (1987). Intracellular transport using microtubule-based motors. *A. Rev. Cell Biol.* **3**, 347–378.
Vandre, D D., Davis, F. M., Rao, P N. and Borisy, G. G. (1986). Distribution of cytoskeletal proteins sharing a conserved phosphorylated epitope. *Eur. J. Cell Biol.* **41**, 72–81.
Vantard, M., Levillers, N., Hill, A.-M., Adoutte, A. and Lambert, A.-M. (1990). Incorporation of *Paramecium* axonemal tubulin into higher plant cells reveals functional sites of microtubule assembly. *Proc. natn. Acad. Sci. U.S.A.* **87**, 8825–8829.
Venverloo, C. J. and Libbenga, K. R. (1987). Regulation of cell division in vacuolated cells. I. The function of nuclear positioning and phragmosome formation. *J. Pl. Physiol.* **131**, 267–284.
Wick, S. M. (1991) Spatial aspects of cytokinesis in plant cells. *Curr. Opin. Cell Biol.* (in press).
Zhang, D., Wadsworth, P. and Hepler, P. K. (1990). Microtubule dynamics in living plant cells: Confocal imaging of microinjected fluorescent brain tubulin. *Proc. natn. Acad. Sci. U.S.A.* **87**, 8820–8824.

(*Received 17 May 1991 – Accepted, in revised form, 2 August 1991*)